

# The Dependence of the Electronic Conductivity of Carbon Molecular Sieve Electrodes on Their Charging States

Elad Pollak,<sup>\*,†</sup> Isaschar Genish,<sup>‡</sup> Gregory Salitra,<sup>†</sup> Abraham Soffer,<sup>†</sup> Lior Klein,<sup>‡</sup> and Doron Aurbach<sup>†</sup>

Department of Chemistry, Bar-Ilan University, Ramat-Gan 52900, Israel, and Department of Physics, Bar-Ilan University, Ramat-Gan 52900, Israel

Received: January 4, 2006; In Final Form: February 27, 2006

The dependence of the electronic conductivity of activated carbon electrodes on their potential in electrolyte solutions was examined. Kapton polymer films underwent carbonization (1000 °C), followed by a mild oxidation process (CO<sub>2</sub> at 900 °C) for various periods of time, to obtain carbons of different pore structures. A specially designed cell was assembled in order to measure the conductivity of carbon electrodes at different potentials in solutions. When the carbon electrodes possessed molecular sieving properties, a remarkable dependence of their conductivity on their charging state was observed. Aqueous electrolyte solutions containing ions of different sizes were used in order to demonstrate this phenomenon. As the average pore size of the activated carbons was larger, their molecular sieving ability was lower, and the dependence of their conductivity on their charging state regained its classical form. This behavior is discussed herein.

## 1. Introduction

Electrical double layer capacitors are an important development in the field of energy storage and conversion.<sup>1</sup> Unlike batteries, where energy conversion is obtained via electrochemical redox reactions, double layer capacitors are based on electrostatic interactions occurring at the electrode–solution interface. A major advantage of electrical double layer capacitors is their reversibility, since electrostatic interactions are much less detrimental to the electrodes' surface structure and to the electrolyte solution, compared to Faradaic red-ox processes.<sup>2</sup> A major drawback to double layer capacitors is their relatively low energy density compared to rechargeable batteries.

The electroadsorption capacity of porous carbon electrodes is a function of their surface area. Huge surface areas can be achieved by the development of a high concentration of small pores. When the pore diameter approaches the size of ions in solutions, the electroadsorption of these electrodes have molecular sieving properties. The average pore size of activated carbons can be increased by a mild burnoff of the carbon material, which is actually an oxidation process. Molecular sieve carbons have been used for gas separation by means of adsorption–desorption cycles.<sup>4</sup> In a previous work, molecular sieve carbon electrodes were used to calibrate the size of ionic species in various solutions.<sup>5</sup>

The dependence of the electronic conductivity of carbon electrodes on their potential, while being in contact with electrolyte solutions, is very interesting. A parabolic-type dependence with a minimum at the point of zero charge is usually obtained.<sup>6</sup> Many types of carbonaceous materials are classified as semiconductors, although not all of their properties resemble those of conventional semiconducting materials.<sup>7</sup> The conductivity of these semiconducting like carbonaceous materi-

als depends on the concentrations and the mobilities of the electrons and the holes in their lattice. Assuming that the mobilities of both charge carriers are similar, the conductivity varies as a function of the concentration of these two-charge carriers. A minimum in the conductivity of semiconducting materials should be measured when the concentration of holes and free electrons is the same. It should be possible to affect the electronic state of activated carbon electrodes by the nature of the adsorption processes that they undergo as a function of their polarization in electrolyte solutions.

The work reported herein is aimed at a study of the electrical behavior of activated, molecular sieving carbon electrodes as a function of different types of adsorption processes that they can undergo in electrolyte solutions.

## 2. Experimental Section

Kapton-based carbons, originating from Kapton films (Pronat Inc., Israel), were produced by temperature-programmed pyrolysis (up to 1000 °C) under high purity nitrogen flow (99.999%, Oxygen & Argon Works, Israel). Activation, which is, in fact, a partial burn off of the carbons that leads to the formation of pores and the development of a high surface area, was performed by CO<sub>2</sub> (99.995%, BOC Gases) at 900 °C, at a flow rate of 500 mL/min. The samples were then cooled under a N<sub>2</sub> flow in order to minimize the possible formation of surface groups at elevated temperatures by reactions between the carbon and the oxygen from the air.

The activated carbons thus obtained should be considered as treated in an inert gas at 900 °C. These are just the well-known conditions for oxygen surface group removal. Thus the resulting carbons are practically free of, or at least very lean in, oxygenated surface groups<sup>8</sup> in comparison with carbons treated with concentrated nitric acid,<sup>9</sup> for example. Carbons with surface areas of several hundreds of square meters per gram were obtained by this activation method. Adsorption isotherms and surface area measurements were obtained by an Autosorb 1

\* To whom correspondence should be addressed: E-mail: ch305@mail.biu.ac.il.

<sup>†</sup> Department of Chemistry.

<sup>‡</sup> Department of Physics.

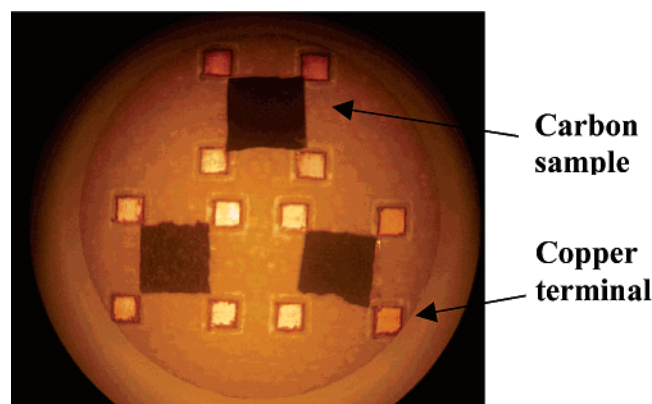


**Figure 1.** Experimental scheme of conductivity vs.  $T$  measurements (before contacting the copper terminals with the carbon sample).

system (Quantachrome Inc.) using nitrogen as an adsorbate at 77 °K (using the BET approach).

The measurement of the dependence of the electrical conductivity on temperature was conducted by a physical property measurement system (PPMS) (Quantum Design). A specially designed set up was used (Figure 1). The carbon sample was held in place by a double-sided adhesive film, and the electrical contacts between the carbon and the copper terminals were made using silver paste (SPI supplies). An ultrasonic wire bonder (West-Bond) was used to make electrical contacts between the copper terminals and the PPMS. The conductivity measurements were conducted at the temperature range between 0.45 and 300 °K. Low temperatures were achieved using liquid  $^3\text{He}$ .

Highly pure salts for the electrolyte solutions were obtained from the following companies: KCl from Frutarom (Israel),  $\text{MgCl}_2$  from Fluka, and  $\text{K}_2\text{SO}_4$  from Sigma-Aldrich. Doubly distilled water was used for the preparation of all electrolyte solutions.

The specific conductivity of the dry carbon electrodes was calculated using the Van der Pauw method.<sup>10</sup>

Figure 2 shows the experimental set up for measurements of the electronic conductivity of carbon electrodes in solutions, as a function of their electrochemical potential: four copper wires were attached to the corners of a rectangular carbon electrode (9 mm  $\times$  9 mm) by means of a conductive silver paste (Figure 2A). An epoxy adhesive (Araldite) was applied in order to attach the carbon electrode to the electrochemical cell. The epoxy adhesive was also applied to the bottom of the carbon electrode in order to improve the strength of the assembly of the electrode and the copper wires. The electrochemical cell was filled with the aqueous solution, which was then purged with high purity nitrogen in order to remove oxygen traces from the solution.

Phase analysis of the carbonized Kapton polymer was obtained by X-ray diffraction, measured by a D8 Advance System (Bruker Inc.), Using  $\text{Cu K}\alpha$  radiation ( $\lambda = 1.54 \text{ \AA}$ ), operated at 40 mA and 40 kV. High-resolution scanning electron microscopy of the carbon samples was performed by a field emission electron microscope (JEOL-JSM-700F).

Cyclic voltammograms (PGSTAT Autolab electrochemical measuring system from Ecco Chemie, Inc. The Netherlands), were measured at a scan rate of 1 mV/sec within the potential range  $-0.4 \text{ V} \rightarrow +0.7 \text{ V}$  vs. a standard calomel electrode (SCE). Prior to each conductivity measurement, the carbon electrodes were cycled at a scan rate of 1 mV/sec, within the above potential range, until steady and reproducible voltammograms were obtained. The electrodes' capacity was calculated from the cyclic voltammograms, using the relation  $C[\text{F/gr}] = (I/\nu)/\text{electrode mass}[\text{gr}]$ , where  $I$  is the current in amperes and  $\nu$  is

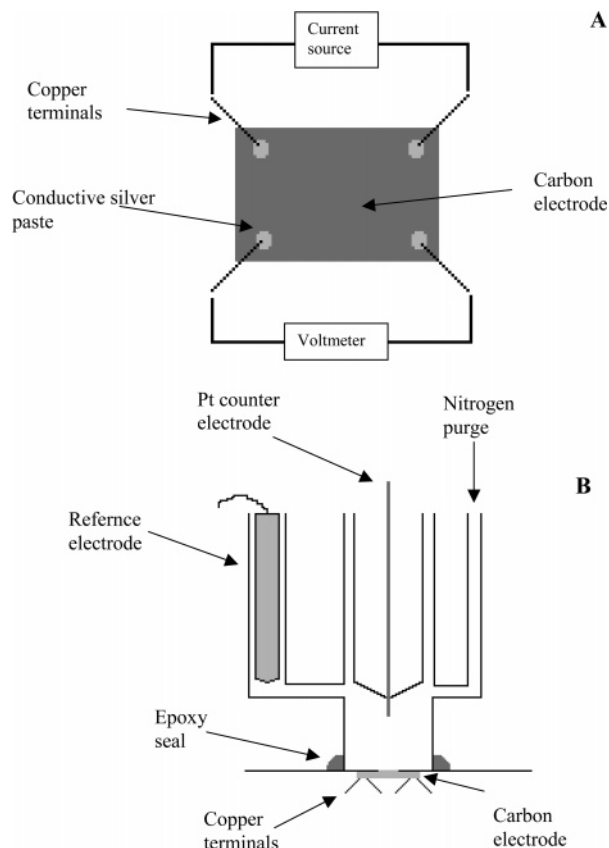


**Figure 2.** Experimental scheme of the conductivity measurements of carbon electrodes at different potentials. A, bottom view. B, side view.

the scan rate in V/sec. Figure 2A shows the conductivity measurements' setup: the carbon electrode potential was set vs the reference electrode. A constant current of 1 mA was supplied (Yokogawa DC source 7651), and the voltage drop across the carbon electrode (less than 1 mV) was measured using a Keithley 2182 nanovoltmeter, and recorded by a PC equipped with LABVIEW 7.0 software. A period of at least 1 h was required at each electrochemical potential in order to ensure that the electrochemically induced current of the carbon electrode is negligible in comparison with the source current used for the conductivity measurement. The carbon electrode conductivity was measured at an electrochemical potential range of  $-0.4 \text{ V} \rightarrow +0.6 \text{ V}$  vs. SCE. It should be noted that the conductivity values presented herein were normalized with respect to the value of the minimal conductivity measured during each experiment.

Impedance spectroscopy measurements were performed in a three-electrode cell. The capacity was calculated from the imaginary part at a frequency of 10 mHz according to  $C = -1/2\pi f Z''$ ,  $f \rightarrow 0$ .

All measurements were conducted at a temperature of 25 °C (room temperature).

### 3. Results and Discussion

The Kapton-based carbons were activated by  $\text{CO}_2$  at 900 °C for periods of 2 and 4 h, and the resulting activated carbons possessed a specific (BET) surface area of 216.7  $\text{m}^2/\text{gr}$  and 441.7  $\text{m}^2/\text{gr}$ , respectively. Specific RT conductivities of the dry (no solution) 2 and 4 h-activated carbon electrodes were 67.3 S/cm and 89.9 S/cm, respectively.

XRD patterns of the differently activated carbon samples, gave the classic pattern of amorphous carbon materials, namely

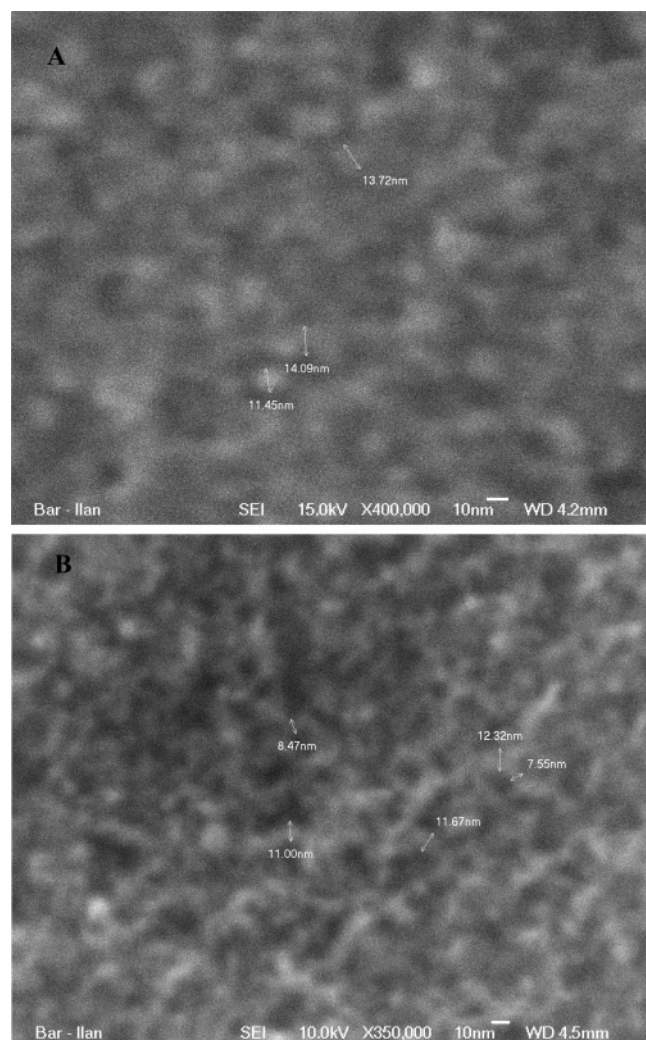


**Figure 3.** HRSEM images of the 2 h (A) and the 4 h (B) activated carbon electrodes.

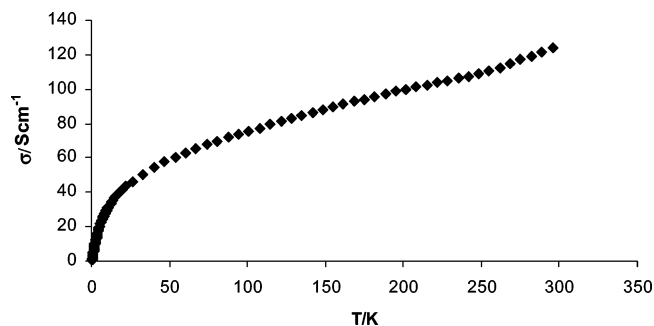


**Figure 4.** Dependence of the conductivity of a typical activated carbon sample on the temperature.

two broad peaks located at  $24^\circ$  and  $44^\circ$ , corresponding to the 002 plane and the 100 plane, respectively.<sup>11</sup> The crystallite size of the 2 and 4 h activated samples was 11.904 Å and 11.152 Å, respectively. The crystallite size was calculated using the well-known Debye–Scherrer formulas.

HRSEM images of the activated carbons are given in Figure 3. It is clearly seen that the average pore wall of the 2 h-activated carbon electrode is somewhat larger than that of the 4 h-activated carbon electrode.

The dependence of the specific conductivity on the temperature is plotted in Figure 4. The increase in the conductivity with temperature is the typical behavior of a semiconductor material. This type of material does not exhibit an Arrhenius

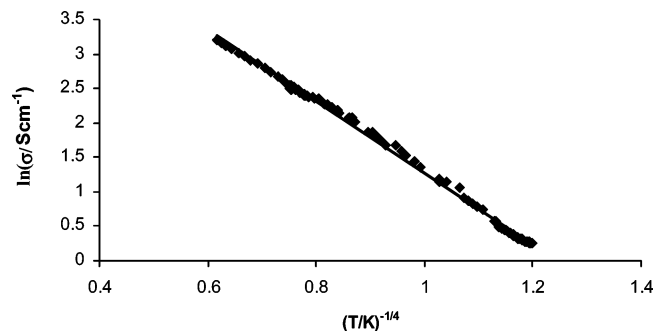


**Figure 5.** Dependence of the conductivity of a typical activated carbon sample on temperature according to the hopping mechanism (solid line-curve fit).

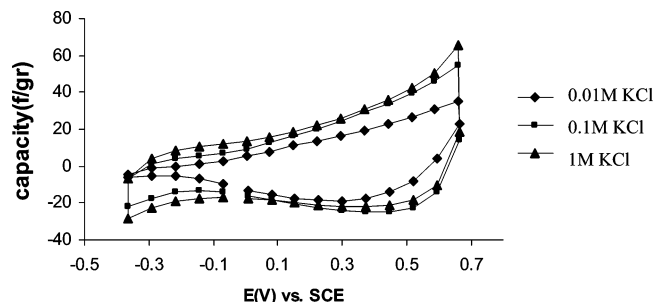
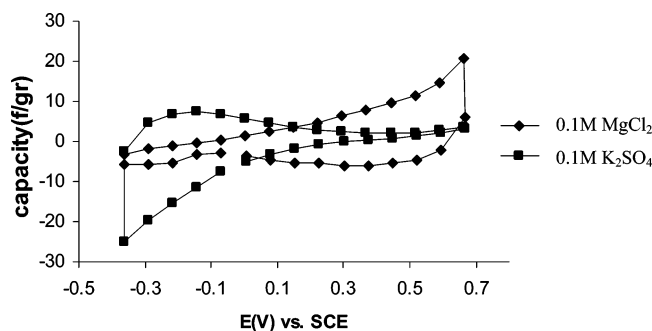


**Figure 6.** Cyclic voltammograms of 2 h activated carbon electrodes solutions containing different concentrations of KCl.

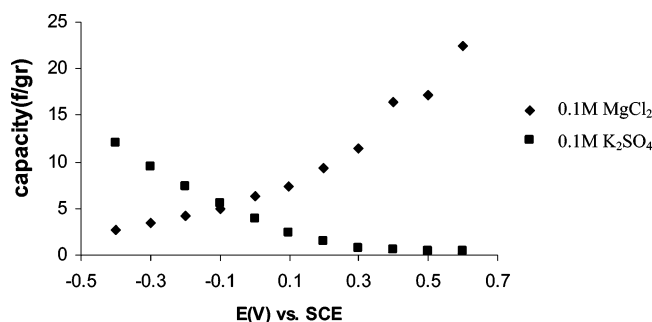
type dependence of the conductivity on the temperature. The dependence of the conductivity on temperature in the range 0.5 °K to 10 °K follows the equation:  $\sigma = A \exp(-BT^{-1/4})$ , where A and B are empirical constants, as demonstrated in Figure 5 (showing  $\ln \sigma$  vs  $T^{-1/4}$ ). This type of dependence at low temperatures, was explained by the hopping mechanism, while at higher temperatures the mechanism is governed by thermal activation.<sup>12,13</sup> According to the hopping model, a few layers of C atoms form a domain, within which the charge is delocalized. Charges can migrate between domains by means of tunneling when the domains are twisted toward one another.

Figure 6 exhibits typical cyclic voltammograms of a 2 h-activated Kapton-based carbon electrode in solutions containing different concentrations of KCl. The PZC of these systems is estimated to be 0.1 V vs SCE, based on immersion potentials<sup>14</sup> measurements and the minimum in the capacity in the relevant impedance measurements.<sup>15</sup> It is noticeable that, at low concentrations of KCl, the carbon electrode exhibits a molecular sieving effect toward  $K^+$ , namely, low currents at negative potentials due to difficulties in the adsorption of  $K^+$  ions and higher currents in the positive potentials related to  $Cl^-$ -ions' adsorption. Upon increasing the KCl concentration, this molecular sieving effect toward  $K^+$  is weakened. On the thermodynamic level, this is most likely due to the higher chemical potential, which forces the cation into the narrow pores. On the molecular level, we propose the following reason for this: at low concentrations, the average distance between the ions is large and, therefore, ions of opposite signs cannot shield each other's charge. As a result, the hydration shell of the cations created by water molecules is quite large, and hence, the effective size of the cations is too large to accommodate the carbon pores. When the salt concentration is high, the distance between oppositely charged ions is small, and thus the hydration cations' shell, that is required for the shielding of the charge, becomes smaller. Hence, the effective size of the ion becomes small enough to accommodate the carbon pores.





**Figure 7.** Cyclic voltammograms of 2 h-activated carbon electrodes in  $\text{MgCl}_2$  and  $\text{K}_2\text{SO}_4$ .



**Figure 8.** Capacity-potential curves obtained from impedance spectroscopy for 2 h-activated carbon electrodes in  $\text{MgCl}_2$  and  $\text{K}_2\text{SO}_4$  solutions.

Figures 7 and 8 show the cyclic voltammograms and capacity-potential curves (obtained using impedance spectroscopy measurements), respectively, of the 2 h-activated electrodes in  $\text{MgCl}_2$  and in  $\text{K}_2\text{SO}_4$  solutions. This electrode exhibits a strong molecular sieving effect toward  $\text{Mg}^{2+}$  (at negative potentials), which is a divalent ion and, therefore, its charge density is rather high in comparison with that of monovalent ions.<sup>5</sup> Therefore, the hydration shell of  $\text{Mg}^{2+}$  is large, resulting in an effective ion size, which is too large to be electro-adsorbed into the carbon pores. The  $\text{SO}_4^{2-}$  ions' solutions exhibit the same molecular sieving effect at potentials positive with respect to the potential of zero charge (PZC), determined also by the minimum in capacity values measured by the impedance measurements. The discrepancy between the capacity obtained from cyclic voltammetry (CV) and that obtained from impedance spectroscopy stems from the kinetics of these electroadsorption processes. When using the CV method, the scan rate plays a major role when dealing with kinetically controlled processes occurring at the electrode interface. The capacity obtained from impedance spectroscopy is equivalent to the capacity derived from a very slow scan rate CV.

Cyclic voltammograms and capacity-potential curves of the 4 h-activated carbon electrode in different concentrations of KCl are shown in Figures 9 and 10, respectively. As can be clearly seen, the molecular sieving effect toward  $\text{K}^+$  has disappeared completely due to pore enlargement created by the more intensive activation process ( $\text{CO}_2$  at  $900^\circ\text{C}$ ). The capacity-potential curve (Figure 10) exhibits a minimum in the capacity at a potential of 0 V vs. SCE, which corresponds to the potential of zero charge. When dealing with  $\text{MgCl}_2$  and  $\text{K}_2\text{SO}_4$  (Figures 11 and 12), it can be seen that the molecular sieve effect toward  $\text{Mg}^{2+}$  (at the negative potentials) and toward  $\text{SO}_4^{2-}$  (at positive potentials) has diminished, yet not completely disappeared due to the large effective size of these divalent ions.

Figure 13 exhibits the dependence of the electronic conductivity of a 2 h-activated carbon electrode on its potential, during

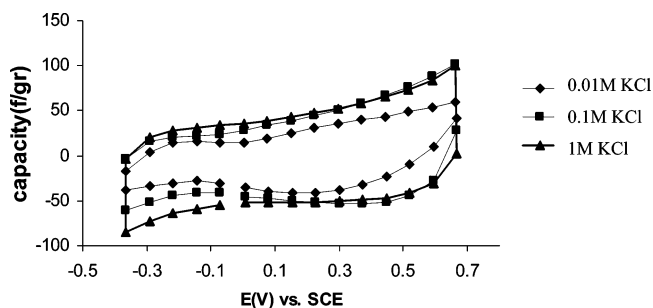


**Figure 9.** Cyclic voltammograms of 4 h-activated carbon electrodes in solutions containing different concentrations of KCl.

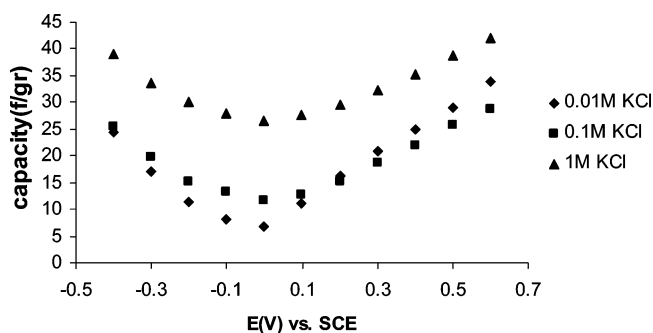


**Figure 10.** Capacity-potential curves obtained from impedance spectroscopy for 4 h-activated carbon electrodes in solutions containing different concentrations of KCl.

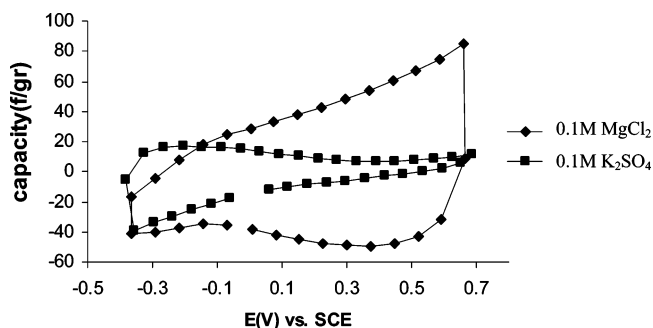


**Figure 11.** Cyclic voltammograms of 4 h-activated carbon electrodes in  $\text{MgCl}_2$  and  $\text{K}_2\text{SO}_4$  solutions.

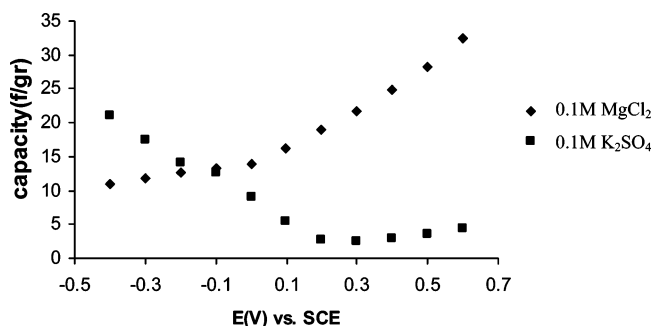


**Figure 12.** Capacity-potential curves obtained from impedance spectroscopy for 4 h-activated carbon electrodes in  $\text{MgCl}_2$  and  $\text{K}_2\text{SO}_4$  solutions.

the polarization of this electrode in different KCl solution (indicated in the figure). This graph shows that when the electrode was polarized anodically (to positive potentials), namely the region of  $\text{Cl}^-$  electroadsorption, the conductivity of the electrode increases with potential, while at negative potentials, the dependence of the electrode's conductivity on potential is invariant. We connect this invariance in conductivity at the low potentials to the fact that, at a low concentration of

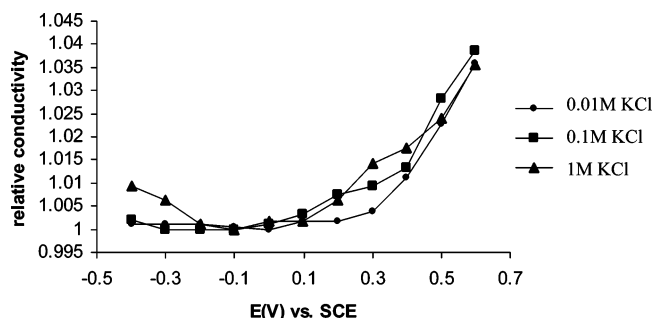


**Figure 13.** Conductivity–potential curves of 2 h-activated carbon electrodes in solutions containing different concentrations of KCl.

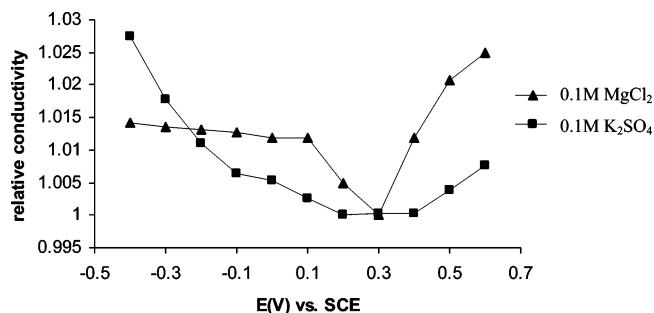


**Figure 14.** Conductivity–potential curves of 2 h-activated carbon electrodes in  $\text{MgCl}_2$  and  $\text{K}_2\text{SO}_4$  solutions.

KCl, no pronounced electroadsorption of the cations is indicated (see Figure 6). As seen in Figure 13, when a 1 M KCl solution was used, the electrical conductivity of the carbon electrode increases, as the cathodic polarization is higher. Indeed, upon increasing the solution concentration, there is more pronounced electroadsorption of  $\text{K}^+$ . The connection between the electrical conductivity of the activated carbon electrodes and the electroadsorption of ions is further demonstrated in solutions containing large ions, such as hydrated  $\text{Mg}^{2+}$  and  $\text{SO}_4^{2-}$ . Figure 14 shows the dependence of the conductivity on the electrode's potential during polarization of 2 h-activated carbon electrodes in  $\text{MgCl}_2$  and  $\text{K}_2\text{SO}_4$  solutions. It can be clearly seen that, at potentials in which the electroadsorption of  $\text{K}^+$  or  $\text{Cl}^-$  is expected, the electrical conductivity increases with polarization, while the scarce electroadsorption of large ions such as  $\text{Mg}^{2+}$  and  $\text{SO}_4^{2-}$  at negative and positive potentials, respectively, is indeed connected to a very little dependence of conductivity vs polarization. These changes in the activated carbon electrodes' conductivity are explained by models for semiconductor type materials developed by Kastening et al.: Upon negative (or positive) polarization of the carbon electrodes, an excess of electrons (or holes) is created in the space-charge layer (near the electrode–solution interface). Cations (or anions) at the solution side migrate to the interface due to electrostatic forces created by the excess of charge at the electrode side of the interface. When the pore size at the surface of the electrode is too small to allow the insertion of cations (or anions), there are not enough species that can balance an excess of charge created at the electrode side of the interface. Hence, in the absence of pronounced electroadsorption, it is impossible to accumulate an excess of charge at the electrode side of the interface. As a result, no changes in the electronic conductivity are observed upon polarization because polarization cannot create an excess of charge at the electrode side. When comparing the electrode's capacity to its conductivity, we see a similar kind of dependence on the electrode potential. This can be explained as follows: the electrode's capacity reflects the possible accumulation of charge at the solution side of the interface. In parallel, the

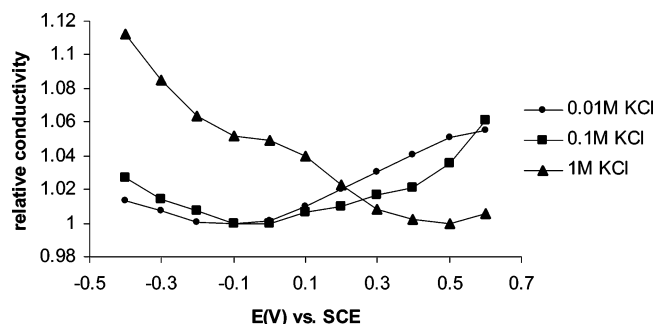


**Figure 15.** Conductivity–potential curves of 4 h-activated carbon electrodes in solutions containing different concentrations of KCl.

conductivity is determined by the amount of charge carriers that exist in the electrode (at the space-charge layer in the present cases).

Upon the enlargement of the average pore size of the activated carbon electrodes (i.e., the use of 4 h-activated carbons), it is clearly seen that the molecular sieving effect discussed above diminishes significantly. This is due to the fact that the large pore diameter enables the electroadsorption of large ions as well when there are no limitations to ion insertion into the carbon's pores, and hence, polarization of the electrodes leads to pronounced electroadsorption. The excess of charge (electrons or holes) created at the electrode's side, due to its polarization, can be well balanced by the charge of the electroadsorbed ions. Thereby, polarization leads to an increase in the conductivity (as the potentials are far, either positive or negative, from the PZC). Figure 15 shows conductivity–potential curves of 4 h-activated carbon electrodes at different concentrations of KCl. At 0.01 M and 0.1 M KCl, both the minimum in the conductivity and the minimum in the capacity fall at the same potential, of 0 V vs SCE. As seen in Figure 15, when the concentration of KCl in solution was 1 M, the most pronounced dependence of the conductivity on the potential (upon cathodic polarization) was measured. This can be explained by the pronounced effect of the electrolyte concentration on the size of the hydration shell of  $\text{K}^+$ , and hence, on the actual size of the cations in this solution. Thus, the pronounced dependence of conductivity vs potential of the 4 h-activated carbons electrodes in the 1 M KCl solution is due to an easy insertion of cations into the carbon pores, and hence, the most effective balance of the electrodes' negative charge by electroadsorption upon cathodic polarization. This enables the creation of a relatively high excess of charge at the electrode's side, thus leading to increased conductivity. It is noticeable that in all the cases measured herein, the changes in the electrodes' conductivity, that were due to polarization, were less than 10% (compared to the lowest value). Kastening et al.<sup>6</sup> and Hahn et al.<sup>15</sup> reported a change of approximately 40% in the conductivity when the electrodes' active material was spherical-shaped activated carbons in the work reported by Kastening et al.<sup>6</sup>. The thickness of the pores' walls of that material was reported to be in the range of 1 nm. This is roughly the thickness of the space-charge layer; hence, the entire solid material comprises the space-charge layer. In the case of the Kapton-based activated carbons used herein, the thickness of the pore walls is much greater. To estimate this thickness, we consider the porous carbon as composed of disordered flat graphite platelets between which the pores are contained. As platelets, their thickness is much smaller than the length and width. Thus the specific surface area (SSA) can be attributed to the flat surface only. Under this approximation, the thickness obeys the following relation:  $\text{SSA} = 2/\rho d$ ,<sup>16</sup> where SSA is the specific surface area in  $\text{cm}^2/\text{gr}$ ,  $\rho$  is the density of the material

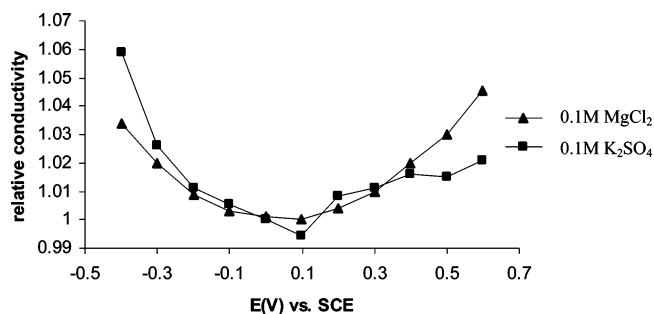


**Figure 16.** Conductivity–potential curves of 4 h-activated carbon electrodes in  $\text{MgCl}_2$  and  $\text{K}_2\text{SO}_4$  solutions.

in  $\text{g}/\text{cm}^3$ , and  $d$  is the thickness of the pore wall in cm. The thicknesses of the 2 and 4 h-activated carbons were calculated as 12.075 and 6.723 nm, respectively. These thicknesses of the pore wall are confirmed by the HR–SEM images (as shown in Figure 3), where, approximately, the same average pore wall thicknesses are measured. Therefore, it is clear that in the case of the Kapton-based activated carbons, the space-charge layer consists of only a small fraction of the total solid material. This is the reason for the lower changes in the electrodes' conductivity upon their polarization, measured in this work. The different behavior of the conductivity vs potential curve in the 1 M KCl solution can be attributed, in part, also to the possible formation of chemical bonds between the anions and the carbon surface, which affects the electronic properties of the carbon  $\text{Cl}^-$  material (e.g., the PZC). This phenomenon is still under study.

From Figure 16 it is evident that the molecular sieve effect observed in  $\text{Mg}^{2+}$  solutions for the 2 h-activated carbon electrodes nearly disappears with the 4 h-activated carbon electrodes, because of their larger, average pore size.

The method described herein, is a further demonstration of the molecular sieving properties of carbon electrodes in the solution phase; until now, the molecular sieving effect of carbon electrodes in solution was demonstrated by electrochemical methods, such as cyclic voltammetry<sup>5</sup> and impedance spectroscopy. In the present work the molecular sieving effect of activated carbon electrodes was also studied via changes of the carbon electrode's electrical conductivity during charging. Unlike cyclic voltammetry and impedance spectroscopy, this method relies on changes in the physical nature of the solid and not on electrochemical changes.

#### 4. Conclusions

The dependence of the electronic conductivity of activated carbon electrodes as a function of potential, while being polarized in various aqueous electrolyte solutions, was measured. When the pores of the activated carbon are too small, and hence, do not allow the electroadsorption of large cations or anions, the electrode's conductivity was found to be nearly potential invariant in the range where electroadsorption was scarce. By increasing the pore size of the activated carbons, their molecular

sieving effect disappears, and then changes in the conductivity were observed as a function of polarization potential, both in the positive and negative potential domains. Hence, when there is no restriction on electroadsorption, and the carbon pores are sufficiently large to accommodate both cations and anions, cathodic or anodic polarization pronouncedly increases the concentration of charge near the electrode's surface. This occurs due to the possibility of neutralization and stabilization of the excess charge near the carbon's surface (electrode's side) by the electroadsorption of ions in the solution side of the interface. Hence, this possibility of charge accumulation upon polarization leads to an increase in the electrode's conductivity as the degree of polarization is higher. This work provides a proof, which does not rely completely on electrochemistry but more on the solid properties of carbonaceous materials, to the existence of the molecular sieving properties of porous carbon electrodes.

#### References and Notes

- (1) Nishino, A. Capacitors: Operating Principles, Current Market and Technical Trends. *J. Power Sources* **1996**, 60 (2), 137–147.
- (2) Yata, S.; Okamoto, E.; Satake, H.; Kobota, H.; Fuji, M.; Taguchi, T.; Kinoshita, H. Polyacene Capacitors. *J. Power Sources* **1996**, 60 (2), 207–212.
- (3) Koresch, J.; Soffer, A. Stereoselectivity in Ion Electroadsorption and in Double-Layer Charging of Molecular Sieve Carbon Electrodes. *J. Electroanal. Chem. Interfacial Electrochem.* **1983**, 147, 223–234.
- (4) Koresch, J. E.; Soffer, A. *Sep. Sci. Technol.* **1983**, 18 (8), 723.
- (5) Eliad, L.; Salitra, G.; Aurbach, D.; Soffer, A. Ion Sieving Effects in the Electrical Double Layer of Porous Carbon Electrodes: Estimating Effective Ion Size in Electrolytic Solutions. *J. Phys. Chem. B* **2001**, 105, 6880–6887.
- (6) Kastening, B. A Model of the Electronic Properties of Activated Carbon. *Phys. Chem. Chem. Phys.* **1998**, 102 (2), 229–237.
- (7) Kastening, B.; Hahn, M.; Kremeskoetter, J. The Double Layer of Activated Carbon Electrodes Part 2. Charge Carriers in Solid Material. *J. Electroanal. Chem.* **1994**, 374 (1), 159–166.
- (8) Salitra, G.; Soffer, A.; Eliad, L.; Cohen, Y.; Aurbach, D. Carbon Electrodes for Double-Layer Capacitors I. Relations Between Ion and Pore Dimensions. *J. Electrochem. Soc.* **2000**, 147 (7), 2486–2493.
- (9) Nian, Y.; Teng, H. Nitric Acid Modification of Activated Carbon Electrodes for Improvement of Electrochemical Capacitance. *J. Electrochem. Soc.* **2002**, 149 (8), A1008–A1014.
- (10) van der Pauw, L. J. A Method of Measuring the Resistivity and Hall Coefficient on Lamellae of Arbitrary Shape. *Philips Tech. Rev.* **1957**, 20, 220–224.
- (11) Endo, M.; Kim, C.; Karaki, T.; Kasai, T.; Matthews, M. J.; Brown, S. D. M.; Dresselhaus, M. S.; Tamaki, T.; Nishimura, Y. Structural Characterization of Milled Mesophase Pitch Based Carbon Fibers. *Carbon* **1998**, 36 (11), 1633–1641.
- (12) Sheng, P.; Klafter, J. Hopping Conductivity in Granular Disordered Systems. *Phys. Rev. B* **1983**, 27, 2583–2586.
- (13) Mott, N. F. *Conduction in Non-Crystalline Materials*; Clarendon Press: Oxford, UK, 1987; p 27 ff.
- (14) Eliad, L.; Salitra, G.; Soffer, A.; Aurbach, D. On the Mechanism of Selective Electroadsorption of Protons in the Pores of Carbon Molecular Sieves. *Langmuir* **2005**, 21, 3198–3202.
- (15) Hahn, M.; Baerteschi, M.; Barbieri, O.; Sauter, J. C.; Kotz, R.; Gally, R. Interfacial Capacitance and Electronic Conductance of Activated Carbon Double-Layer Electrodes. *Electrochem. Solid-State Lett.* **2004**, 7 (2), A33–A36.
- (16) Fung, A. W. P.; Dresselhaus, M. S.; Endo, M. Transport Properties Near the Metal–Insulator Transition in Heat Treated Activated Carbon Fibers. *Phys. Rev. B* **1993**, 48 (20), 14953–14962.